J. Serb. Chem. Soc. 84 (9) 1027–1039 (2019) UDC 546.284–31:544.773.43:620.266.1
JSCS–5244 *Original scientific paper*

Hybrid mesoporous silica with controlled drug release

LÁSZLÓ ALMÁSY[1,2]*, ANA-MARIA PUTZ[3]**, QIANG TIAN[1], GENNADY P. KOPITSA[4,5], TAMARA V. KHAMOVA[5], RÉKA BARABÁS[6], MELINDA RIGÓ[6], ATTILA BÓTA[7], ANDRÁS WACHA[7], MARIUS MIRICA[8], BOGDAN ŢĂRANU[8] and CECILIA SAVII[3]

[1]State Key Laboratory of Environment-Friendly Energy Materials, Southwest University of Science and Technology, Mianyang 621010, China, [2]Institute for Solid State Physics and Optics, Wigner Research Centre for Physics, Hungarian Academy of Sciences, POB 49 Budapest 1525, Hungary, [3]"Coriolan Drăgulescu" Institute of Chemistry Timisoara of Romanian Academy, Bv. Mihai Viteazul, No. 24, RO-300223, Timisoara, Romania, [4]Institute of Silicate Chemistry of RAS, nab. Makarova 2, 199034 St. Petersburg, Russia, [5]Petersburg Nuclear Physics Institute, PNPI 1, Orlova roscha mcr., Gatchina, Leningrad region, 188300, Russia, [6]Babeş-Bolyai University, Faculty of Chemistry and Chemical Engineering, Department of Chemistry and Chemical Engineering of Hungarian Line of Study, Arany Janos Str. No. 11, RO-400028, Cluj-Napoca, Romania, [7]Research Centre for Natural Sciences, Hungarian Academy of Sciences, Budapest 1519 Budapest, POB 286, Budapest-1117, Hungary and [8]National Institute for Research and Development in Electrochemistry and Condensed Matter, Dr. Aurel Păunescu Podeanu Str. No. 144, RO-300569, Timisoara, Romania

(Received 9 November 2018, revised 16 January, accepted 24 January 2019)

Abstract: The mesoporous silica particles were prepared by the sol–gel method in one-step synthesis, in acidic conditions, from tetraethoxysilane (TEOS) and methyltriethoxysilane (MTES), varying the mole ratio of the silica precursors. Nitric acid was used as catalyst at room temperature and hexadecyltrimethyl ammonium bromide (CTAB) as structure directing agent. Optical properties, porosity and microstructure of the materials in function of the MTES/TEOS ratio were evaluated using infrared spectroscopy, nitrogen adsorption and small angle X-ray scattering. All materials showed the ordered pore structure and the high specific surfaces, making them suitable as the drug delivery systems. Drug loading and release tests using ketoprofen were performed to assess their performance for drug delivery applications. The amount of the methylated precursor used in the synthesis had little effect on the drug loading capacity, but had a strong influence on the initial rate of the drug release.

Keywords: sol–gel process; ketoprofen; hybrid material; SAXS.

*,** Corresponding authors. E-mail: (*)almasy@mail.kfki.hu, (**)lacramaanamaria@yahoo.com
https://doi.org/10.2298/JSC181109009A

INTRODUCTION

Mesoporous silica with ordered pore structure can be synthesized using ionic surfactants as directing agents, with alkaline or acidic catalysts. The alkaline route involves direct co-condensation of anionic inorganic species with a cationic surfactant, by self-assembly of anionic silicates and cationic surfactant molecules.[1] Such synthesis often requires high temperature and a long reaction time, in order to obtain ordered pore arrangement.[2]

Silica with ordered mesoporosity can also be prepared in acidic conditions. The advantage of acidic medium is that high quality mesoporous silica can be obtained in a short duration reaction, at room temperature.[3] The acid anion from the catalyst buffers the repulsion between the cationic silicate species and the ammonium surfactant, by means of the weak hydrogen bonding forces in acidic conditions. In that way, the acidic pathway can offer more flexible structures and morphologies than the alkaline pathway, due to weaker surfactant/silicate interaction.[2]

The ordered mesoporous material is formed from the pre-existing surfactant liquid crystal phase and the micelles are subsequently coated with the slowly condensing silica.[4] Cubic, lamellar and hexagonal structures can be produced in ways predictable from surfactant–water phase diagrams, and the morphology can be changed by variation of the mixture composition or processing temperature.[5] The degree of ordering and the pore size can be changed by varying the chain length of the surfactant molecule, or using co-solvent additives.[6,7,8]

Another way to manipulate the pore structure and the pore surface is to use mixed precursors. The attempts of using methylsilane as partial substituent for TEOS resulted in the increase of the surface area, to the significant decrease of the pore size and to the broadening of the pore size distribution.[9,10] Also, the materials stable over time toward water can be obtained due to the enhancement of the surface hydrophobicity induced by increased density of the surface methyl groups.[11] Under the acidic condition, the rate of MTES hydrolysis/polymerization is much greater than that of TEOS. Comparatively, under the alkaline conditions, the hydrolysis-polymerization rate of MTES decreases noticeably.[12,13] We have recently reported the morphology development of mesoporous MCM-41 materials prepared with mixtures of MTES and TEOS in alkaline synthesis conditions and the obtained hexagonally ordered structure from pure TEOS to equimolar MTES–TEOS ratio.[14]

Since the first demonstration by Vallet-Regí *et al.* of using MCM-41 type mesoporous silica as drug carriers,[7] this class of materials has been extensively explored for drug loading and release properties.[15–30] The key parameters that affect the adsorption and the release of organic molecules are the particle size, the pore size, and the chemical nature of the pore surface. In order to be suitable for biomedical use the materials must be biocompatible, non-toxic, have an open

pore network, be homogenous in size, and have large surface area. Surfactant--templated mesoporous silica fulfils all these conditions. Furthermore, the large variety of particle types, synthesis methods and surface modifications make them useful for drug delivery applications. Control of the drug loading and subsequent release can be achieved by the functionalization of the silanol groups on the pore surface.[28] Besides the more complex synthesis procedure, there are also drawbacks of the post-synthesis functionalization, because of the non-even coverage of the pore surfaces by the attached groups, or even blocking the pore entrances, especially in materials with relatively small pore sizes such as MCM-41.[29]

In studies of mesoporous silica particles used as drug carriers, either the performance of the prepared original material is analyzed, or particles having different geometries,[16,22,26,27,29] pore sizes,[7,15,26,29] or functionalized with different molecular groups,[17–21,25,29] are compared. While for developing materials with the required release performance, the common approach is to find a suitable functionalization, there is a shortage of studies in which the release properties are fine-tuned by the continuous variation of the pore morphology or pore surface hydrophobicity.

We prepared MCM-41 mesoporous hybrid silica materials using mixed silica precursors, and hexadecyl trimethyl ammonium bromides (CTAB) as templating agent. HNO_3 was chosen as catalyst, based on its favourable performance observed in comparative studies.[2,31] The pore morphology was changed by adding methyltriethoxysilane (MTES) in different concentrations into the reaction medium. The resulting drug adsorption and the release performance depend on the pore structure, a continuous variation of which offers a possibility to fine tune the release profiles. The prepared mesoporous silica samples have been tested as drug delivery systems; drug loading and release measurements have been performed.

As model molecule, ketoprofen (2-(3-benzoylphenyl)propionic acid) has been chosen, which is an anti-inflammatory analgesic and antipyretic drug, used in treatment of acute pain and chronic arthritis.[32] The main difficulty associated with the commercial formulation is the poor water solubility, which leads to poor dissolution rate and a subsequent decrease in its gastrointestinal absorption,[33] and the significant drug loss and possible damaged healthy organs and tissues. The drawbacks of the commercial ketoprofen formulations with rapid release are that the peak plasma levels occur within 0.5–2 h and a rapid clearance after 1–4 h, giving limited effectiveness and fluctuating plasma drug concentration.[34] Finding the carrier materials with control of the drug release rate is therefore a primary goal for improving the performance of ketoprofen carrier formulations.

The presented one-pot synthesis demonstrates a simple way of preparation and control of morphology and drug release properties of hybrid mesoporous silica.

EXPERIMENTAL

Synthesis

All chemicals were commercially available: tetraethoxysilane (TEOS, 99 %, for analysis, Fluka); methyltriethoxysilane (MTES, 97 %, Merck); hexadecyltrimethyl ammonium bromide (CTAB, Sigma); nitric acid (Merck, 65 % HNO_3).

Materials were synthesized under acidic conditions following a modified recipe of Xiang by using the CTAB directing agent.[2] The TEOS precursor was partially substituted by MTES in different mole ratios, such as, MTES:TEOS = 0:10; 1:9; 2:8; 3:7; 4:6; 5:5. The mole ratio of the reactants was: (TEOS+MTES):CTAB:H_2O:HNO_3 = 3:1:741:18.7. First, 5.47 g of CTAB was dissolved in a nitric acid solution (19.42 mL of 65 % HNO_3 in 195.66 mL H_2O). The mixtures were vigorously stirred at 40 °C for at least 30 min. Then, the sol–gel precursors (10 mL TEOS or TEOS+MTES mixed in advance) were slowly dripped (within 10 min) into the reaction mixture and the stirring continued for 3 h (rotation speed 300 rpm) at 40 °C. The formed gel was aged for one day, in static condition. On the following day, the white precipitate was washed several times with distilled water until the pH of the supernatant approached the pH value of the distilled water. Subsequently, the samples were filtered and dried in air at room temperature for one day, and then at 100 °C. Afterwards, the samples were thermally treated at 550 °C for 6 h (heating at 1 °C/min) to remove the directing agent and were labelled as: C*x*, where *x* is a number from 0 (no MTES content) to 5 (the highest MTES content).

Characterization

FTIR spectra were taken on KBr pellets with a JASCO-FT/IR-4200 apparatus. Samples after drying as well as after calcination have been studied.

Measurements of specific surface area were performed by low temperature nitrogen adsorption using QuantaChrome Nova 1200e analyzer. Before measurements the samples were outgassed at 120 °C for 17–18 h in vacuum. Surface area, S_{BET}, has been determined by Brunauer–Emmett–Teller (BET) method. The pore sizes have been calculated by the Barrett––Joyner–Halenda (BJH) method from the adsorption branches of the isotherms. The analysis of the pore size distribution was performed on the basis of nitrogen adsorption isotherms using DFT method (cylindrical pore, NLDFT adsorption branch model).

Small-angle X-ray scattering measurements were conducted on the CREDO laboratory instrument, operating with point focus geometry.[35] The scattering intensity $I(q)$ was recorded as a function of scattering vector $q = 4\pi\sin(\theta/\lambda)$, where λ is the wavelength of the incident radiation, and θ is half of the scattering angle. CuKα radiation of 0.154 nm wavelength from a the microfocus anode source was used. A Pilatus 300K two-dimensional CMOS detector with pixel size of 0.172 mm was placed at a distance of 337 mm from the sample, covering a q-range of 0.4–8 nm^{-1}, which is well suited to observe the first three or four diffraction peaks of MCM-41 type materials. The scattering intensity was azimuthally averaged over the detector, and the data were corrected and normalized by measurement time, transmission, sample thickness, background subtraction, and geometrical distortions.

Drug loading and release tests

Ketoprofen has been used as the active pharmacologic agent. It has been loaded into the 6 samples by dissolution in ethanol[36] at 17 g/L. For drug loading, 100 mg of silica carrier was put in 5 mL of ethanol solution. After 24 h, the material was filtered and left to dry at room temperature for another day. Afterwards, the drug loaded material was weighed and the amount of the adsorbed drug was determined from the mass increase.

For the release experiment, the ketoprofene-loaded silica powders were pressed to pastilles. The simulated body fluid (SBF) solution was prepared using Kokubo recipe,[37] and left to rest in the laboratory for one day, in order to check for occasional precipitate formation. Then it was divided for setting up a calibration curve, and for the release media of the 6 samples. Its pH was 7.2, mimicking the intestinal fluid. The ketoprofen concentration in SBF was followed by measuring the UV absorbance at 260 nm. For the desorption experiment, a sample was soaked in 20 mL of SBF.[19] At the regular time intervals, 2 mL of liquid was removed for analysis, and replaced by SBF. The dissolution experiment was performed at room temperature, 23 °C.

RESULTS AND DISCUSSION

FT-IR spectra

The FT-IR spectra reveal the characteristic bands for the methylated silica materials (Fig. 1). Bands of the OH stretching vibrations of adsorbed water were noticed around 3440 cm^{-1}.[38] Their intensities are decreasing with the increase of MTES content, indicating the increase of the hydrophobicity of the material.

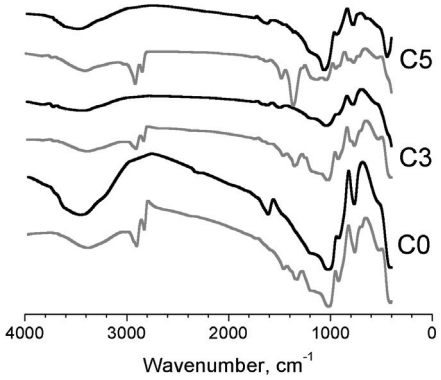

Fig. 1. FT-IR spectra of the xerogels (gray lines) and the thermally treated samples (black lines).

All samples showed the specific vibration bands assigned to the silica skeleton at 1050, 800 and 450 cm^{-1}, corresponding to the asymmetric stretching, symmetric stretching and bending vibration of the Si–O–Si network, respectively.[38] The presence of the silanol groups was confirmed by the existence of the band centred about 960 cm^{-1}, which is associated with the stretching mode of the Si–OH groups.

The characteristic vibration bands of the organic groups of the surfactant molecules and the bands of the methyl groups from MTES precursor are at: 2930, 2860, 1760, 1509, 1488, 1387, 1350 and 1139 cm^{-1}. The CH stretching vibrations for saturated aliphatic species occur between 3000 and 2800 cm^{-1} (bands at 2930 and 2860 cm^{-1} are the asymmetric and symmetric CH stretching vibrations)[39] and the corresponding simple bending vibrations occur between 1500 and 1300 cm^{-1}; the asymmetric vibration band of the methyl group at 1365 cm^{-1} is visible in xerogel samples only.[13]

Nitrogen adsorption

The nitrogen adsorption isotherms are typical for MCM-41 type porous materials (Fig. 2a). With the increase of MTES content, the specific surface area (S_{BET}) first increases until 3:7 MTES:TEOS mole ratio, reaching a maximum value 1580 m^2/g, then decreases to 888 m^2/g for the highest MTES content (Table I). With the increase of MTES content, the total pore volume and the pore size are decreasing. The C0 sample shows an isotherm of IV type with hysteresis, and for the MTES containing samples, the isotherms are of IV type, with no hysteresis; the only exception is the material with the highest MTES content, which does not show the distinct capillary condensation step and it probably belongs to type II, characteristic for microporous materials.

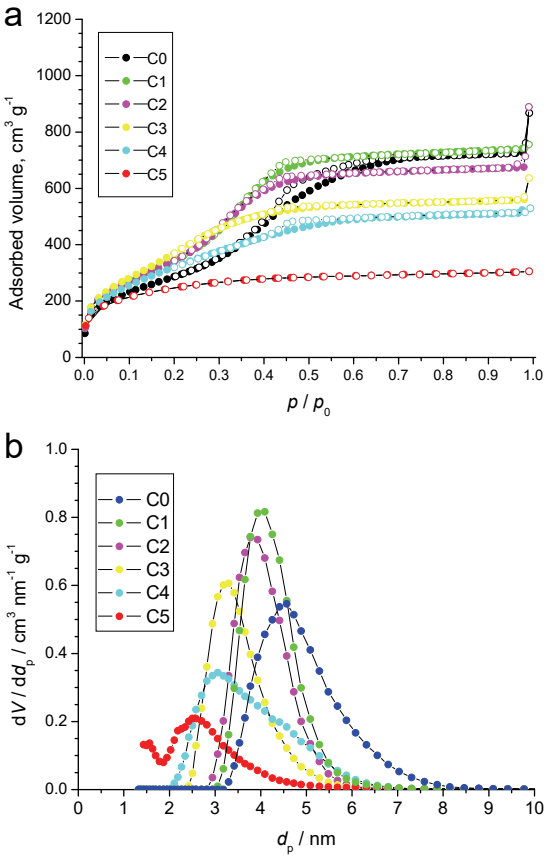

Fig. 2. a) Nitrogen adsorption/desorption isotherms of the hybrid silica samples. b) Pore size distributions calculated by DFT method.

The isotherms are characteristic for MCM-41 type materials with the elongated pores,[40–42] showing a capillary condensation step around p/p_0 of 0.3–0.4 for almost all samples. With the increasing MTES content, the pore size distribution

is shifting toward lower pore dimensions, and becomes broader (Fig. 2b). For all samples, the pore sizes and the high specific surfaces are comparable with the best MCM-41 type mesoporous silica materials, showing that using MTES in synthesis does not reduce strongly their surface, relevant for their drug carrier usage.

TABLE I. Specific surface area, pore diameters and pore volumes obtained by nitrogen porosimetry

Sample	C0	C1	C2	C3	C4	C5
S_{BET} / m^2g^{-1}	1105	1330	1326	1580	1222	888
$d_{P(BJH)}$ / nm	2.95	2.85	2.64	2.10	1.94	2.05
V_T / cm^3g^{-1}	1.183	1.104	1.137	0.863	0.766	0.446
$d_{P(DFT)}$ / nm	4.57	4.09	3.78	3.30	3.06	2.50

Small-angle X-ray scattering

The morphology of mesoporous materials on a nanometer scale can be assessed by the combination of electron microscopy with scattering methods.[43] While the electron microscopy can reveal the structure of porous silica materials at nm resolution in the direct space on a selected part of the sample, the small angle scattering provides the statistically accurate volume-averaged structural information about the whole sample. The SAXS diffractograms are shown in Fig. 3. They exhibit the first three diffraction peaks characteristic for the hexagonal mesoporous structure of surfactant templated MCM-41 type materials[7,14].

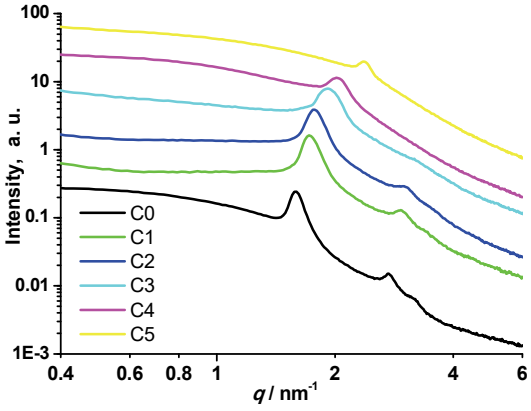

Fig. 3. SAXS scattering curves of the mesoporous silica samples.

For the sample prepared with TEOS only, (sample C0), the first peak is seen at the lowest angles. With the increasing MTES content, the peaks shift to higher angles, indicating that the addition of the hydrophobic precursor leads to the shrinkage of the lattice spacing, and thinning of the silica frame of the pore walls.[14] Such behaviour suggests that the increasing of the methyl content lowers the stability of the structure against mechanical or thermal stress. For the samples

C4 and C5 only the first diffraction peak is observable, showing the gradual loss of the long-range structural order.[8]

Electron microscopy

At low magnification, all samples show the typical particle shapes of the ordered mesoporous silica prepared in acidic conditions.[6] They appear as folded or twisted rope fibres at lower magnification (Fig. 4).

At high magnification, the arrays of very long tubules are observed, which correspond to the hexagonally ordered pore structure of typical MCM-41 materials.

Evaluation of Ketoprofen loading capacity and release profile

Drug loading. The main factors influencing the drug loading and release are the surface area, the pore dimensions and the chemical composition of the surface.

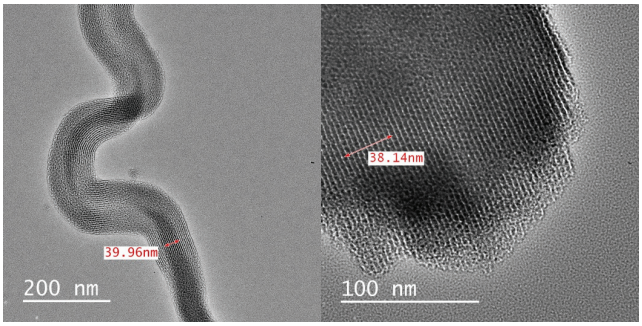

Fig. 4. TEM images of silica particles for sample C0.

The surface area is the most determining factor for the amount of the adsorbed drug. The adsorption is governed by the size selectivity related to the compatibility of the size of drug molecules to the pore dimensions. The drug loading can therefore be modified by the increasing/decreasing the surface area and the pore size, and by changing the surface-drug affinity.

The pore volumes in the series of hybrid samples decreased from 1.19 to 0.45 cm^3/g with increasing MTES content, and the pore surface decreased from 1100 to 900 m^2/g (Table I). The ketoprofen loading capacities in the given conditions were between 45 and 80 % (Table II). For most of the samples, the loading capacity does not change systematically, and it stays within 20 % range in average. In another study where the surface functionalization of mesoporous silica was realised by the post-grafting with trimethylmethoxysilane, the modification resulted in the decreased surface area, the pore size, and the pore volume, which decreased the flurbiprofen-loading capacity by about 50 %.[44] Authors explained it by the decreased pore volume after functionalization.

In mesoporous silica, the drug–pore wall interaction is influenced by the atomic groups at the surface[45] and also by the weak drug-drug interactions at

higher pore filling.[28] The pore size distribution also influences the drug loading: the adsorption in large pores is more efficient than in smaller ones, due to the faster diffusion,[46] but on the other hand for materials with larger pores the specific surface is smaller. Considering that the adsorption is favoured by the interaction of the carboxylic (–COOH) functional group of ketoprofen with the superficial hydroxylic (OH) groups of silica, a hydrophobic silica surface provides less active sites for adsorption, resulting in lower loading capacity.[46]

TABLE II. Ketoprofen loading and release in hybrid mesoporous silica samples

Loading and release	C0	C1	C2	C3	C4	C5
Loading in silica, wt.%	67.0	65.9	66.5	67.5	73.7	70.6
Release after 1 h, wt.%	8.8	9.8	6.1	4.0	3.4	4.3
Release after 24 h, wt.%	17.4	11.7	8.4	5.3	10.9	5.2

In vitro *drug release.* Dissolution of ketoprofen in the SBF is displayed in Fig. 5 as the cumulative weight percentage of the drug released in time.

The cumulative release data have been fitted to the theoretical and the empirical equations of zero and first order kinetics, Higuchi model, Hixson–Crowell model and Korsmeyer–Peppas model.[47,48]

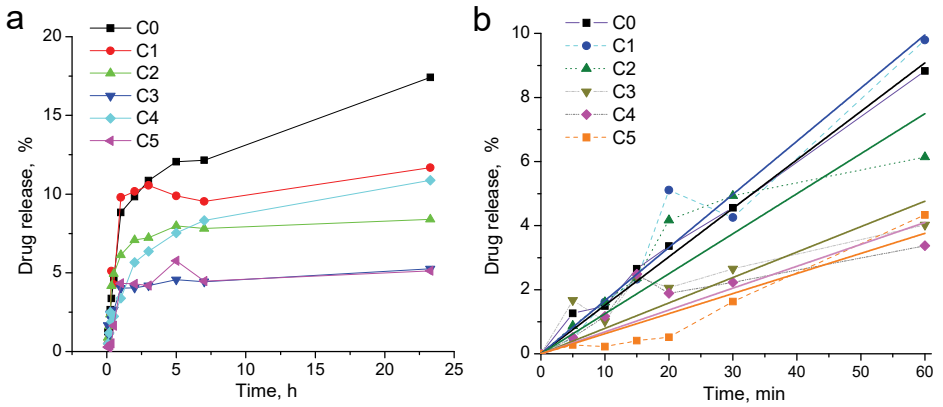

Fig. 5. Ketoprofen release profiles in SBF. Straight solid lines are zero order kinetics fitted to the first hour data.

All they showed the reasonable fits to the first hour data, while the fit quality got worse over the 24 h interval. The coefficients of determination (R^2) of the aforementioned models applied to the 24 h data were between 0.85 and 0.98 varying non-systematically between the samples. For the comparison between the samples in function of their methyl content, the first hour release data were fitted by the zero order kinetics, describing processes with the concentration independent release rates. The coefficients of determination were between 0.94 and 0.99, and the results are shown in Fig. 5b. The retarding effect of the used mixed pre-

cursors for the hybrid silica is clearly seen, with about twofold decrease of the release rate from the C0 to the C5 samples.

The release properties of the different samples can also be assessed by comparing the quantities of the ketoprofen released after 1 and 24 h, as shown in Table II. For the C5 sample, the released amount was approximately two times lower than for C0 after one hour, and three times lower after 24 h. The modification of the pore surface by hydrophobic groups can lead to various results, depending on the nature of the drug molecule, and the type of the silica matrix. In the comprehensive studies with larger hydrophobic molecular groups, Doadrio *et al.* could vary the drug release rate by an order of magnitude, using different alkyl chains grafted in large pore SBA-15 silica matrix.[19] Behaviour similar to our results has been observed recently by Yilmaz *et al.*[44] Large pore mesoporous SBA-15 silica with methyl groups attached by post-grafting with trimethylmethoxysilane, showed slower release rates when compared to the non-functionalized sample.[44] The functionalization of the MCM-41 channels with aminopropyl groups, by post-grafting, led to the strong decrease of the release rate.[49] Since the drug binding occurs mainly by the hydrophobic attraction between the drug and the alkyl moieties in the pore channels, in the case of small groups such as methyl, its impact to the drug binding strength can be comparable to the effects caused by the change of the pore size and morphology. During the calcination, most of methyl groups are removed from the surface, therefore the change of the release rate can be attributed to the change of the pore morphology, namely to the decrease of the pore diameter with the increasing proportion of MTES.

CONCLUSION

Mesoporous silica materials have been prepared using mixed MTES and TEOS precursors in acidic conditions and analyzed for their morphology and drug loading and release properties. Increasing the amount of the methyl precursor caused the shrinkage of the hexagonally ordered mesoporous structure and a reduction of the pore diameters, while the total pore volumes and the surface areas remained high and suitable for drug incorporation. Ketoprofen loading and the release tests showed that with the increase of the amount of the functionalized precursor, the loading capacity does not change significantly. However, the drug release rates are strongly affected: for the silica prepared with the largest amount of the methylated precursor the initial release rate is about twice slower, when compared to the material made of pure TEOS. This study presents a simple and efficient method of control of the drug release properties within a certain range in mesoporous hybrid silica materials with the ordered pore structure.

Acknowledgement. Authors thank the Romanian Academy and the Inter-Academic Exchange Program between Romanian Academy and the Hungarian Academy of Sciences.

ИЗВОД

ХИБРИДНЕ МЕЗОПОРОЗНЕ SiO_2 ЧЕСТИЦЕ ЗА КОНТРОЛИСАНО ОТПУШТАЊЕ ЛЕКОВА

LÁSZLÓ ALMÁSY[1,2], ANA-MARIA PUTZ[3], QIANG TIAN[1], GENNADY P. KOPITSA[4,5], TAMARA V. KHAMOVA[5], RÉKA BARABÁS[6], MELINDA RIGÓ[6], ATTILA BÓTA[7], ANDRÁS WACHA[7], MARIUS MIRICA[8], BOGDAN ŢĂRANU[8] и CECILIA SAVII[3]

[1]State Key Laboratory of Environment-Friendly Energy Materials, Southwest University of Science and Technology, Mianyang 621010, China, [2]Institute for Solid State Physics and Optics, Wigner Research Centre for Physics, Hungarian Academy of Sciences, POB 49 Budapest 1525, Hungary, [3]"Coriolan Drăgulescu" Institute of Chemistry Timisoara of Romanian Academy, Bv. Mihai Viteazul, No. 24, RO-300223, Timisoara, Romania, [4]Institute of Silicate Chemistry of RAS, nab. Makarova 2, 199034 St. Petersburg, Russia, [5]Petersburg Nuclear Physics Institute, PNPI 1, Orlova roscha mcr., Gatchina, Leningrad region, 188300, Russia, [6]Babeş-Bolyai University, Faculty of Chemistry and Chemical Engineering, Department of Chemistry and Chemical Engineering of Hungarian Line of Study, Arany Janos Str. No. 11, RO-400028, Cluj-Napoca, Romania, [7]Research Centre for Natural Sciences, Hungarian Academy of Sciences, Budapest 1519 Budapest, POB 286, Budapest-1117, Hungary и [8]National Institute for Research and Development in Electrochemistry and Condensed Matter, Dr. Aurel Păunescu Podeanu Str. No. 144, RO-300569, Timisoara, Romania

Мезопорозне SiO_2 честице су синтетисане сол-гел поступком у једном кораку, у киселим условима, полазећи од тетраетоксисилана (TEOS) и метилтриетоксисилана (MTES), варирањем моларног односа прекурсора силицијума. Као катализатор на собној температури коришћена је азотна киселина, а хексадецилтриметиламонијум-бромид (CTAB) је коришћен као агенс за контролу структуре. Оптичка својства, порозност и микроструктура материјала у функцији односа MTES/TEOS су праћени коришћењем инфрацрвене спектроскопије, адсорпције азота и дифракције X-зрака при малим угловима. Сви материјали су показали уређену порозну структуру и високу специфичну површину, што их чини погодним за системе за контролисано отпуштање лекова. Тестови наношења и отпуштања лека кетопрофена су изведени да би се утврдиле перформансе ових материјала за контролисано отпуштање лекова. Количина метилтриетоксисилана у синтези је имала мали утицај на капацитет везивања лека, али је имала велики утицај на почетну брзину отпуштања лека.

(Примљено 9. новембра 2018, ревидирано 16. јануара, прихваћено 24. јануара 2019)

REFERENCES

1. Q. Huo, D. I. Margolese, U. Ciesla, P. Feng, T. E. Gier, P. Sieger, R. Leon, P. M. Petroff, F. Schüth, G. D. Stucky, *Nature* **368** (1994) 317 (https://dx.doi.org/10.1038/368317a0)
2. W.-D. Xiang, Y.-X. Yang, J.-L. Zheng, L. Cao, H.-J. Ding, X.-N. Liu, *Mater. Sci. – Poland* **28** (2010) 709 (http://www.materialsscience.pwr.wroc.pl/bi/vol28no3/articles/ms_12_2010-051xiang.pdf)
3. Q. Huo, D. I. Margolese, U. Ciesla, D. G. Demuth, P. Feng, T. E. Gier, B. F. Chmelka, F. Schüth, G. D. Stucky, *Chem. Mater.* **6** (1994) 1176 (https://doi.org/10.1021/cm00044a016)
4. M. E. Raimondi, J. M. Seddon, *Liq. Cryst.* **26** (1999) 305 (https://doi.org/10.1080/026782999205100)
5. M. Losurdo, M. M. Giangregorio, G. Bruno, F. Poli, L. Armelao, E. Tondello, *Sensors Actuators, B: Chem.* **126** (2007) 168 (https://doi.org/10.1016/j.snb.2006.11.030)
6. Y. Yu-Xiang, Y. Hai-Ping, S. Jian-Guo, H. Zheng, L. Xiang-Nong, C. Ya-Ru, *J. Am. Ceram. Soc.* **90** (2007) 3460 (https://dx.doi.org/10.1111/j.1551-2916.2007.01951.x)
7. M. Vallet-Regi, A. Rámila, R. P. del Real, J. Pérez-Pariente, *Chem. Mater.* **13** (2001) 308 (https://dx.doi.org/10.1021/cm0011559)

8. A.-M. Putz, C. Savii, C. Ianăşi, Z. Dudás, N. K. Székely, J. Plocek, P. Sfârloagă, L. Săcărescu, L. Almásy, *J. Porous Mater*. **22** (2015) 321 (https://dx.doi.org/10.1007/s10934-014-9899-z)
9. L. Viau, M.-A. Néouze, C. Biolley, S. Volland, D. Brevet, P. Gaveau, P. Dieudonné, A. Galarneau, A. Vioux, *Chem. Mater*. **24** (2012) 3128 (https://dx.doi.org/10.1021/cm301083r)
10. M. M. Rabbani, W.-T. Oh, D.-G. Nam, *Trans. Electr. Electron. Mater.* **12** (2011) 119 (https://doi.org/10.4313/TEEM.2011.12.3.119)
11. M.-A. Néouze, J. Le Bideau, P. Gaveau, S. Bellayer, A. Vioux, *Chem. Mater*. **18** (2006) 3931 (https://dx.doi.org/10.1021/cm060656c)
12. M. J. van Bommel, T. N. M. Bernards, A. H. Boonstra, *J. Non-Cryst. Solids* **128** (1991) 231 (https://doi.org/10.1016/0022-3093(91)90461-E)
13. Y.-F. Wen, K. Wang, P.-H. Pi, J.-X. Yang, Z.-Q. Cai, L.-j. Zhang, Y. Qian, Z.-R. Yang, D.-f. Zheng, J. Cheng, *Appl. Surf. Sci*. **258** (2011) 991 (https://dx.doi.org/10.1016/j.apsusc.2011.06.085)
14. A.-M. Putz, K. Wang, A. Len, J. Plocek, P. Bezdicka, G. P. Kopitsa, T. V. Khamova, C. Ianăşi, L. Săcărescu, Z. Mitróová, C. Savii, M. Yan, L. Almásy, *Appl. Surf. Sci*. **424** (2017) 275 (https://dx.doi.org/10.1016/j.apsusc.2017.04.121)
15. W. Xu, Q. Gao, Y. Xua, D. Wu, Y. Sun, W. Shen, F. Deng, *Powder Technol*. **191** (2009) 13 (https://doi.org/10.1016/j.powtec.2008.09.001)
16. L. Ochiuz, M. C. Luca, I. Stoleriu, M. Moscalu, D. Timofte, G. Tantaru, A. Stefanache, *Farmacia* **64** (2016) 131 (http://www.revistafarmacia.ro/201601/issue12016art21.html)
17. G. Maria, D. Berger, S. Nastase, I. Luta, *Micropor. Mesopor. Mater*. **149** (2012) 25 (https://doi.org/10.1016/j.micromeso.2011.09.005)
18. G. Maria, A.-I. Stoica, I. Luta, D. Stirbet, G. L. Radu, *Micropor. Mesopor. Mater*. **162** (2012) 80 (https://doi.org/10.1016/j.micromeso.2012.06.013)
19. J. C. Doadrio, E. M. B. Sousa, I. Izquierdo-Barba, A. L. Doadrio, J. Perez-Pariente, M. Vallet-Regí, *J. Mater. Chem.* **16** (2006) 462 (https://dx.doi.org/10.1039/B510101H)
20. P. Horcajada, A. Rámila, G. Férey, M. Vallet-Regí, *Solid State Sci*. **8** (2006) 1243 (https://doi.org/10.1016/j.solidstatesciences.2006.04.016)
21. C. O. Arean, M. J. Vesga, J. B. Parra, M. R. Delgado, *Ceram. Int*. **39** (2013) 7407 (https://doi.org/10.1016/j.ceramint.2013.02.084)
22. M. B. M. Al Tameemi, D. Gudovan, R. Stan, D. Mihăiescu, C. Ott, *Romanian J. Mater*. **45** (2015) 188 (http://solacolu.chim.upb.ro/p188-193web.pdf)
23. S. Bhattacharyya, G. Lelong, M.-L. Saboungi, *J. Exp. Nanosci*. **1** (2006) 375 (https://doi.org/10.1080/17458080600812757)
24. A. L. Doadrio, A. J. Salinas, J. M. Sánchez-Montero, M. Vallet-Regí, *Curr. Pharm. Des*. **21** (2015) 6189 (https://doi.org/10.2174/1381612822666151106121419)
25. M. Popova, I. Trendafilova, Á. Szegedi, D. Momekova, J. Mihály, G. Momekov, L. F. Kiss, K. Lázár, N. Koseva, *Micropor. Mesopor. Mater*. **263** (2018) 96 (https://doi.org/10.1016/j.micromeso.2017.12.005)
26. S. Nastase, L. Bajenaru, C. Matei, R. A. Mitran, D. Berger, *Micropor. Mesopor. Mater*. **182** (2013) 32 (https://doi.org/10.1016/j.micromeso.2013.08.018)
27. M. Petrescu, R.-A. Mitran, C. Matei, D. Berger, *Rev. Roum. Chim.* **61** (2016) 557 (http://revroum.lew.ro/wp-content/uploads/2016/06/Art%2011.pdf)
28. M. Vallet-Regi, F. Balas, D. Arcos, *Angew. Chem. Int. Ed*. **46** (2007) 7548 (https://doi.org/10.1002/anie.200604488)

29. H. Ritter, J. H. Ramm, D. Brühwiler, *Materials* **3** (2010) 4500 (https://doi.org/10.3390/ma3084500)
30. N. Ž. Knežević, G. N. Kaluđerović, *Nanoscale* **9** (2017) 12821 (https://dx.doi.org/10.1039/C7nr04445C)
31. R. Ryoo, J. M. Kim, C. H. Ko, C. H. Shin, *J. Phys. Chem*. **100** (1996) 17718 (https://dx.doi.org/10.1021/jp9620835)
32. A. Abd-Elbary, M. A. El Nabarawi, D. H. Hassen, A. A. Taha, *Int. J. Pharm. Pharm. Sci*. **6** (2014) 183 (https://innovareacademics.in/journals/index.php/ijpps/article/view/2041)
33. N. A. Martin, J. S. Patrick, *Phys. Pharm. Pharm. Sci.,* Lippincott Williams & Wilkins, New York, 2006, 4th ed., pp. 212–213
34. *Ketoprofen*, https://pubchem.ncbi.nlm.nih.gov/compound/ketoprofen
35. A. Wacha, Z. Varga, A. Bóta, *J. Appl. Cryst*. **47** (2014) 1749 (https://doi.org/10.1107/S1600576714019918)
36. C. Charnay, S. Bégu, C. Tourné-Peteilh, L. Nicole, D. A. Lerner, J. M. Devoisselle, *Eur. J. Pharm. Biopharm.* **57** (2004) 533 (https://doi.org/10.1016/j.ejpb.2003.12.007)
37. *Simulated body fluid*, http://mswebs.naist.jp/LABs/tanihara/ohtsuki/SBF/
38. R. Al-Oweini, H. El-Rassy, *J. Mol. Struct.* **919** (2009) 140 (https://doi.org/10.1016/j.molstruc.2008.08.025)
39. J. M. Berquier, L. Teyssedre, C. Jacquiod, *J. Sol–Gel Sci. Technol*. **13** (1998) 739 (https://doi.org/10.1023/A:1008609525830)
40. M. Grün, I. Lauer, K. K. Unger, *Adv. Mater*. **9** (1997) 254 (https://doi.org/10.1002/adma.19970090317)
41. M. Grün, K. K. Unger, A. Matsumoto, K. Tsutsumi, *Micropor. Mesopor. Mater*. **27** (1999) 207 (https://doi.org/10.1016/S1387-1811(98)00255-8)
42. M. Kruk, M. Jaroniec, A. Sayari, *Langmuir* **13** (1997) 6267 (https://doi.org/10.1021/la970776m)
43. B. Pauwels, G. Van Tendeloo, C. Thoelen, W. Van Rhijn, P. A. Jacobs, *Adv. Mater.* **13** (2001) 1317 (https://doi.org/10.1002/1521-4095(200109)13:17<1317::AID-ADMA1317>3.0.CO;2-5)
44. M. S. Yilmaz, A. Palantoken, S. Piskin, *J. Non-Cryst. Solids* **437** (2016) 80 (https://doi.org/10.1016/j.jnoncrysol.2016.01.020)
45. M. Colilla, F. Balas, M. Manzano, M. Vallet-Regí, *Solid State Sci*. **10** (2008) 408 (https://doi.org/10.1016/j.solidstatesciences.2007.12.009)
46. S. Smirnova, S. Suttiruengwong, W. Arlt, *KONA Powder Part. J.* **23** (2005) 86 (https://doi.org/10.14356/kona.2005012)
47. G. Singhvi, M. Singh, *Int. J. Pharm. Stud. Res.* **2** (2011) 77 (http://technicaljournalsonline.com/ijpsr/)
48. A. Kierys, P. Krasucka, M. Grochowicz, *Saudi Pharm. J.* **25** (2017) 972 (https://dx.doi.org/10.1016/j.jsps.2017.03.004)
49. Y. Zhang, Z. Zhi, T. Jiang, J. Zhang, Z. Wang, S. Wang, *J. Control. Release* **145** (2010) 257 (https://dx.doi.org/10.1016/j.jconrel.2010.04.029).